Mutational Analysis of Novel Effector Domains in Rac1 Involved in the Activation of Nicotinamide Adenine Dinucleotide Phosphate (Reduced) Oxidase†

Amir Toporik,‡ Yara Gorzalczany,‡ Miriam Hirshberg,§ Edgar Pick,‡ and Ofra Lotan*,‡

The Julius Friedrich Cohnheim-Minerva Center for Phagocyte Research, Department of Human Microbiology, Sackler School of Medicine, Tel Aviv University, Tel Aviv 69978, Israel, and Division of Protein Structure, The National Institute for Medical Research, Mill Hill, London NW7 1AA, United Kingdom

Received January 6, 1998; Revised Manuscript Received March 3, 1998

ABSTRACT: The small molecular weight GTP-binding protein Rac (1 or 2) is an obligatory participant in the activation of the superoxide-generating NADPH oxidase. Active NADPH oxidase can be reconstituted in a cell-free system, consisting of phagocyte-derived membranes, containing cytochrome b_{559}, and the recombinant cytosolic proteins p47-*phox*, p67-*phox*, and Rac, supplemented with an anionic amphiphile as an activator. The cell-free system was used before for the analysis of structural requirements of individual components participating in the assembly of NADPH oxidase. In earlier work, we mapped four previously unidentified domains in Rac1, encompassing residues 73−81 (***a***), 103−107 (***b***), 123−133 (***c***), and 163−169 (***d***), as important for cell-free NADPH oxidase activation. The domains were defined by assessing the activation inhibitory effect of a series of overlapping peptides, spanning the entire length of Rac1 [Joseph, G., and Pick, E. (1995) *J. Biol. Chem. 270*, 29079−29082]. We now used the construction of Rac1/H-Ras chimeras, domain deletion, and point mutations, to ascertain the functional relevance of three domains (***b***, ***c***, and ***d***) predicted by "peptide walking" and to determine the importance of specific residues within these domains. This methodology firmly establishes the involvement of domains ***b*** and ***d*** in the activation of NADPH oxidase by Rac1 and identifies H103 and K166, respectively, as residues critical for the effector function of these two domains. The functional significance of domain ***c*** (insert region) could not be confirmed, as shown by the minor effect of deleting this domain on NADPH oxidase activation. Analysis of the three-dimensional structure of Rac1 reveals that residues H103 and K166 are exposed on the surface of the molecule. Modeling of the activity-impairing point mutations suggests that the effect on the ability to activate NADPH oxidase depends on the side chains of the mutated amino acids and not on changes in the global structure of the protein. In conclusion, we demonstrate the existence of two novel effector sites in Rac1, necessary for supporting NADPH oxidase activation, supplementing the canonical N-terminal effector region.

Professional phagocytes use oxygen-derived radicals as a main defense mechanism against invading pathogens. The primordial oxygen radical, superoxide (O_2^-),[1] is generated by the action of a multimeric enzyme, known as the NADPH oxidase, which utilizes one-electron reduction of molecular oxygen, at the expense of NADPH. The NADPH oxidase is comprised of a membranal heterodimeric flavocytochrome (cytochrome b_{559}), which consists of two polypeptides (gp91-*phox* and p22-*phox*), and three cytosolic components, p47-*phox*, p67-*phox*, and Rac (1 or 2). The enzyme is latent in resting cells and, upon activation by a variety of stimuli, the cytosolic components translocate to the plasma membrane to generate the active form of the NADPH oxidase complex, through multiple binding interactions between the individual components (reviewed in refs *1*−*4*).

Two interlinked lines of study helped to elucidate the complexity of the oxidase. One was the development of a cell-free method for activating the NADPH oxidase, consisting, in its elementary form, of membrane and cytosol derived from resting cells (*5*, *6*) and, in its more advanced version, of highly purified or recombinant components (*7*, *8*), supplemented with a critical concentration of an anionic amphiphile. The second was the analysis of phagocytes from patients with chronic granulomatous disease. These cells fail to exhibit NADPH oxidase activity due to the absence or functional deficiencies of cytochrome b_{559}, p47-*phox*, or p67-*phox* (reviewed in ref *9*).

In the course of studies utilizing the cell-free methodology, it was noted that a mixture of p47-*phox* and p67-*phox* could not replace total cytosol, leading to the description and purification (*10*) of a third cytosolic component. In parallel,

† Supported by the Julius Friedrich Cohnheim-Minerva Center for Phagocyte Research, The Israel Science Foundation (Grant 10/94) and the David and Natalie Roberts Chair in Immunopharmacology.

* To whom correspondence should be addressed: Department of Human Microbiology, Sackler School of Medicine, Tel Aviv University, Tel Aviv 69978, Israel. Telephone: 972-3-640-9078. FAX: 972-3-642-9119.

‡ Tel Aviv University.

§ National Institute for Medical Research, London.

[1] Abbreviations: O_2^-, superoxide; *phox*, phagocytic oxidase; Rho-GDI, guanosine 5′-diphosphate dissociation inhibitor for Rho; WT, wild type; GDPβS, guanosine 5′-(2-*O*-thiodiphosphate); GTPγS, guanosine 5′-(3-*O*-thiotriphosphate); PCR, polymerase chain reaction; IPTG, isopropyl β-D-thiogalactopyranoside; LiDS, lithium dodecyl sulfate; GAP, guanosine triphosphatase activating protein.

S0006-2960(98)00040-3 CCC: $15.00
Published on Web 05/02/1998

it was reported that O_2^- production in the cell-free system was enhanced by nonhydrolyzable GTP derivatives (*11*−*13*). It was next found that this is due to the involvement of a GTP-binding protein, identified as Rac1 in guinea pig macrophages (*14*) and Rac2 in human neutrophils (*15*−*17*). The two proteins exhibit 92% homology in their amino acid sequence (*18*). Both Rac1 (*14*, *19*) and Rac2 (*17*, *20*) were isolated from phagocyte cytosol as a complex with the regulatory protein GDP dissociation inhibitor for Rho (RhoGDI), the dimer being identical to what was originally described as the third cytosolic component. Evidence was presented for translocation of Rac to the membrane, upon cell activation, consequent to its dissociation from RhoGDI (*21*, *22*), but both the occurrence of translocation (*23*) and its relevance to oxidase activation (*24*) are controversial. The relationship of Rac translocation to that of the other cytosolic components (*25*−*30*) and the role of cytochrome b_{559} in the membrane association of Rac (*28*) are unsettled issues. In both in vitro and in vivo studies, it was found that Rac binds to p67-*phox* in a GTP-dependent manner, suggesting that p67-*phox* represents the principal target of Rac in the course of NADPH oxidase activation (*31*−*34*).

Several investigations, utilizing the cell-free system, dealt with the structure−function relationship of Rac in NADPH oxidase activation. Rac and Ras are only 30% homologous and have distinct biological roles; however, small GTP binding proteins belonging to the Ras superfamily were shown to share a common three-dimensional structure and possess similar mechanisms of action (reviewed in ref *35*). The first studies were based on the paradigm established by mutagenesis studies performed with Ras. These led to the identification of single residues important for NADPH oxidase activation, between amino acids 26 and 45 (N26, A27, F28, G30, I33, T35, V36, D38, Y40, and M45), a region that is analogous to the N-terminal effector region of Ras (*31*, *36*, *37*). Another approach used analysis of chimeric proteins of Rac with members of the Rho subfamily. Amino acids sequence alignment of these proteins reveals high homology with Rac (∼70%); however, these proteins are either incapable of activating or are poor activators of the NADPH oxidase. Studies with Rac1/Cdc42Hs (*38*) and Rac1/RhoA (*39*) chimeras confirmed the importance of the N-terminal effector site but also revealed the existence of a C-terminal effector region, encompassing residues 143−175 (*39*). It was observed that mutations in both the N-terminal and the C-terminal effector regions impaired Rac binding to p67-*phox* (*31*, *34*, *39*). Sequence alignment of Ras with proteins of the Rho subfamily reveals a 13 amino acid insert region, characteristic for Rho proteins (*40*). It was reported that deletion of and point mutations within the insert region in Rac reduced its ability to activate NADPH oxidase (*41*) but did not affect binding to p67-*phox* (*34*).

A different methodology to identify regions in Rac1, important for NADPH oxidase activation, was based on the use of synthetic peptides corresponding to the C-terminal sequence of Rac1. This method provided evidence for the importance of the polybasic motif at the carboxyl tail of Rac1 (*42*, *43*), and this was supported by studies using C-terminal truncation and point mutations converting basic residues to neutral or acidic residues (*44*). Recently, a systematic approach to the use of synthetic peptides for structure−function studies was introduced, based on assessing the NADPH oxidase inhibitory effect of 90 overlapping pentadecapeptides, spanning the entire length of Rac1 (*45*). This method, designated "peptide walking", revealed five domains important for NADPH oxidase activation: the C-terminal polybasic region and four new domains, not identified before. To further investigate the role of these domains and to identify essential residues within the domains, we used generation of Rac1/H-Ras chimeras, domain deletion, and single amino acid mutagenesis. The present report firmly establishes the critical role of two domains in the C-terminal half of Rac1 and of specific residues within these domains in the NADPH oxidase activating function of Rac1.

EXPERIMENTAL PROCEDURES

Materials. The following chemicals were obtained from Sigma: NADPH (tetrasodium salt, 95% pure), ferricytochrome *c* (from horse heart, 95% pure), FAD (disodium salt), thrombin (from human plasma), bovine serum albumin (fraction V, 96% pure), glutathione immobilized on cross-linked 4% beaded agarose, and guanosine 5′-(2-*O*-thiodiphosphate) (GDPβS). Guanosine 5′-(3-*O*-thiotriphosphate) (GTPγS), polymerase chain reaction (PCR) kit with Pow DNA polymerase, PCR product purification kit, plasmid isolation kit, rapid DNA ligation kit with T4 DNA ligase, and protease inhibitor cocktail (Complete) were purchased from Boehringer Mannheim. *n*-Octyl β-D-glucopyranoside (octyl glucoside) was obtained from Pfanstiehl Laboratories. Isopropyl β-D-thiogalactopyranoside (IPTG) was obtained form MBI Fermentas. Max efficiency DH5α competent *Escherichia coli* cells, *Bam*HI, and *Eco*RI were purchased from Gibco BRL. BA85 0.45 μm pore size nitrocellulose filters were obtained from Schleicher & Schuell. [^{35}S]-GTPγS (1134 Ci/mmol, 1 mCi/mL) was obtained from Amersham Life Science. Lithium dodecyl sulfate (LiDS) and common laboratory chemicals (at the highest purity available) were purchased from Merck.

Mutagenesis. Generation of mutations in Rac1 was performed by sequential PCR mutagenesis (*46*), applied on the Rac1 cDNA, cloned in the bacterial expression vector pGEX-2T at *Bam*HI/*Eco*RI sites (a kind gift of Dr. Thomas L. Leto, National Institutes of Health, Bethesda, MD). Briefly, two fragments, 5′ and 3′ of the mutation to be introduced, were separately PCR-amplified using the endogenous forward and reverse pGEX-2T flanking primers and a pair of complementary designed primers, containing the nucleotide substitutions to be introduced. The two fragments encompassing the desired mutation were annealed and amplified by a subsequent PCR step, using only the endogenous forward and reverse pGEX-2T primers. The resulting DNA fragment was digested with *Eco*RI and *Bam*HI, ligated into pGEX-2T vector, and transformed into competent *E. coli* DH5α cells. All mutated cDNA clones were sequenced by the dideoxy method, verifying the insertion of the mutations.

Preparation of Solubilized Macrophage Plasma Membranes. Subcellular fractions were obtained from guinea pig peritoneal macrophages (*19*). Membranes were solubilized in 40 mM octyl glucoside, freed of octyl glucoside by dialysis, and processed as described previously (*47*). Cytochrome b_{559} concentration in solubilized macrophage plasma membranes was determined as described previously (*47*).

Preparation of Recombinant Rac1 Proteins. Rac1 proteins [wild type (WT) and mutants] were expressed as fusion proteins, linked at their N-termini to glutathione *S*-transferase. Proteins were purified from IPTG-induced *E. coli* cells, using glutathione immobilized on cross-linked beaded agarose, and released by thrombin cleavage (*17*). GTPγS- or GDPβS-bound forms of Rac1 proteins were prepared essentially as described previously (*14*). Before nucleotide exchange, the proteins were brought to a concentration of 0.2 mg/mL and supplemented with 1 mg/mL bovine serum albumin. For exchange, Rac1 proteins were incubated for 30 min at 30 °C with a 20-fold molar excess of GTPγS or GDPβS in 20 mM Tris-HCl (pH 7.5), 150 mM NaCl, 7.2 mM EDTA and 4 mM $MgCl_2$ ($[Mg^{2+}_{free}] = 0.5\ \mu M$). The nucleotide loading was stopped by the addition of $MgCl_2$ to a final concentration of 30 mM ($[Mg^{2+}_{free}] = 22.8$ mM).

Preparation of Baculovirus-Derived p47-phox and p67-phox. Baculoviruses carrying cDNAs for human p47-*phox* and p67-*phox* were kind gifts of Dr. Thomas L. Leto. Suspension cultures of Sf9 cells (2×10^6 cells/mL), grown in serum-free medium (SF-900 II SFM, Life Technologies), were infected with the recombinant baculoviruses and harvested 72 h after infection. The recombinant proteins were purified by a modification (*48*) of the procedure of Leto et al. (*49*).

[^{35}S]GTPγS Binding. This was performed by the nitrocellulose filter assay (*50*), essentially as described in ref *51*.

Assay for Cell-Free Activation of NADPH Oxidase. O_2^- generation assays were performed in 96-well microplates, in final volumes of 202−210 μL. Reaction mixtures consisted of, in order of addition, 2−10 μL of WT or mutated Rac1 protein (resulting in final concentrations of 1−450 nM) preloaded with GTPγS, 10 μL of a mixture composed of p47-*phox* and p67-*phox* (final concentration 20 nM, for each protein, unless otherwise stated) and solubilized macrophage membranes (resulting in a final concentration of cytochrome b_{559} of 5 nM), and 190 μL of assay buffer (65 mM sodium−potassium-phosphate (pH 7.0), 2 mM NaN_3, 1 mM EGTA, 1 mM $MgCl_2$, and 10 μM FAD), containing 200 μM cytochrome *c* and 130 μM LiDS as an activator. Following 90 s of incubation, catalysis was initiated by addition of NADPH (final concentration of 250 μM). O_2^- generation was measured by following the rate of superoxide dismutase-inhibitable cytochrome *c* reduction at 550 nm, in a kinetic assay consisting of 28 measurements at 11 s intervals, performed in a SpectraMax 340 microplate reader (Molecular Devices), using SOFTmax PRO software. An extinction coefficient of 21 $mM^{-1}\ cm^{-1}$ was used to calculate the amount of cytochrome *c* reduced.

Rac1 Kinetic Parameters. O_2^- production-related kinetic parameters of Rac1 proteins were determined by measuring maximal rates of cytochrome *c* reduction at increasing concentrations of Rac1 proteins. Data in milli-OD units per minute were taken from the linear portion of the absorbance curves and converted to moles of O_2^- per mole of cytochrome b_{559} per second. Low rates of O_2^- production, seen in the absence of Rac1 proteins, were subtracted form the rates obtained in the presence of Rac1 proteins. V_{max} (maximal O_2^- generation) and EC_{50} (effective concentration of Rac1 proteins at 50% of V_{max}) were determined using a nonlinear least-squares regression fit of the data to the Michaelis−Menten equation, calculated and plotted using Sigma Plot, version 2.0 (Jandel Scientific).

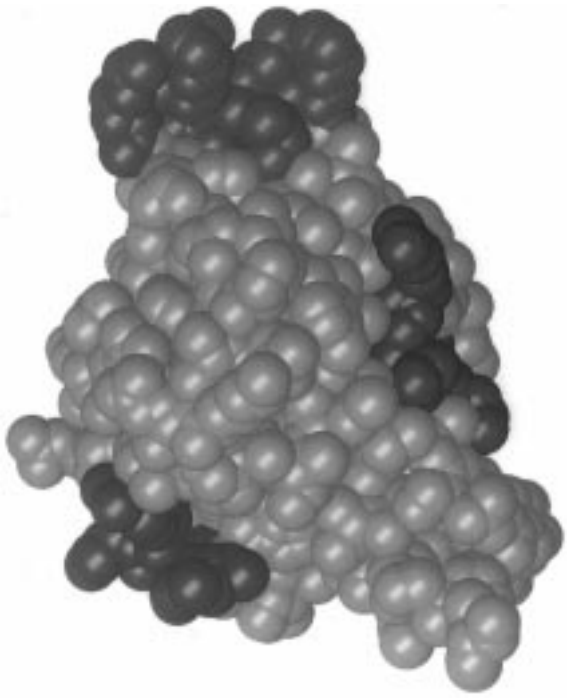

FIGURE 1: Space-filling model (CPK) of WT Rac1 showing domains ***b***, ***c***, and ***d*** in green, cyan, and red, respectively. The figure was generated with Bobscript (*74*).

Protein Quantitation and Electrophoresis. The concentrations of NADPH oxidase cytosolic components were determined by the method of Bradford (*52*), modified for use with 96-well microplates (Technical Bulletin 1177EG, Bio-Rad), using bovine serum albumin as a standard. The purity and integrity of recombinant proteins were analyzed by SDS−polyacrylamide gel electrophoresis, using staining with Coomassie Blue (*10*). The batches of p47-*phox* and p67-*phox* used in the NADPH oxidase activity assays were 99% and 90% pure, respectively.

Model Building. Models of the single-point mutants for both domains ***b*** and ***d*** were constructed from the Rac1 WT structure (*53*), using both CARA (*54*) and SEGMOD (*55*) algorithms within the package LOOK (*56*). For each mutant, both algorithms gave similar structures. As a control, we have mutated each mutant back to WT, which resulted in WT models similar to the actual WT structure. The structures of Cdc42Hs and RhoA were generated using the SEGMOD algorithm (*55*). These structures were recently determined by X-ray crystallography, as complexes with RhoGAP (*57*, *58*). Comparison between the models and the X-ray structures showed the models to be a good representation of the actual three-dimensional structures.

RESULTS

Low molecular mass GTP-binding proteins exhibit a high degree of amino acid sequence homology and share an overall three-dimensional structure (*40*, *53*). To assess the contribution of Rac1 domains defined by "peptide walking" (*45*) to NADPH oxidase activation, these domains (Figure 1) were substituted for their corresponding domains in H-Ras (*40*), prior to the determination of the crystal structure of Rac1 (*53*), as detailed in Table 1. Single amino acid

Table 1: Definition and GTPγS Binding Capabilities of Mutated Rac1 Proteins[a]

nomenclature of Rac1 mutants[b]	amino acids in Rac1	substituted for	domain definition by "peptide walking" [c]	GTPγS binding[d] (mol of GTPγS/ mol of protein)
Rac1(WT)				0.84 ± 0.05[e]
Rac1(G12V)	G_{12}	V		0.72 ± 0.10
Rac1(Y40K)	Y_{40}	K		0.77 ± 0.08
Rac1(***b*** → H-Ras)	$_{103}$HHCPN$_{107}$	$_{104}$VKDSDD$_{109}$[f]	***b***	0.71 ± 0.08
Rac1(***b*** → GAGAG)	$_{103}$HHCPN$_{107}$	GAGAG	***b***	0.79 ± 0.17
Rac1(H103A)	H_{103}	A		0.94 ± 0.01
Rac1(H104A)	H_{104}	A		0.76 ± 0.06
Rac1(C105A)	C_{105}	A		0.93 ± 0.14
Rac1(N107D)	N_{107}	D		0.87 ± 0.06
Rac1(Δ***c***)	$_{123}$KDTIEKLKEKK$_{133}$	A	***c***	0.90 ± 0.05
Rac1(***d*** → H-Ras)	$_{163}$RGLKTV$_{168}$	$_{150}$QGVEDA$_{155}$[f]	***d***	0.75 ± 0.04
Rac1(R163D)	R_{163}	D		0.89 ± 0.08
Rac1(K166E)	K_{166}	E		0.75 ± 0.10
Rac1(T167E)	T_{167}	E		0.86 ± 0.14
Rac1(***control*** → H-Ras)	$_{135}$TPITYP$_{140}$	$_{123}$RTVESR$_{128}$[f]		0.65 ± 0.13

[a] Rac1 proteins (WT and mutants) were generated and purified as described in Experimental Procedures. [b] The nomenclature of Rac1 mutations was guided by the convenience of writing; details of the corresponding domain substitutions and point mutations are presented in columns 2 and 3 of this table. [c] Domains mutated in this work were previously defined by the inhibitory effect of overlapping peptides from the primary sequence of Rac1 on NADPH oxidase activation, and the nomenclature presented in column 4 corresponds to that appearing in the original paper (*45*). [d] Guanine nucleotide-binding assays were performed by the nitrocellulose filter assay at low concentrations of free Mg^{2+} (0.5 μM) using [^{35}S]GTPγS, as described in Experimental Procedures. [e] Data are presented as molar ratios of GTPγS to Rac1 proteins and represent the mean of at least four experiments ± SEM. [f] Regions in H-Ras (*40*) corresponding to the regions in Rac1 defined by "peptide walking"; numbers represent the position of the amino acids in the H-Ras sequence.

mutagenesis was used to complement the findings derived by substitutions of the entire domains.

Characterization of Mutated Rac1 Proteins. Rac1 proteins (WT and mutants) were 95% pure, as judged by Coomassie Blue-stained polyacrylamide gels, and had an apparent molecular mass of 22 000 Da. The only exception was the Rac1(Δ***c***) mutant, which exhibited a molecular mass of approximately 21 000 Da, corresponding to the deletion of 10 amino acids (data not shown).

The stability of Rac1 proteins, considered as an indicator of proper folding (*59*), was estimated by comparing the yields of soluble proteins isolated from *E. coli* cytosol. Most of the Rac1 proteins were purified with yields similar to native Rac1, except for the Rac1(***b*** → H-Ras) chimera, which was recovered in low yields, indicative of improper folding (data not shown). However, sufficient quantities of Rac1(***b*** → H-Ras) were obtained to perform functional assays.

To establish that differences in NADPH oxidase activation were not due to variations in GTPγS binding capacity, [^{35}S]-GTPγS binding assays were performed. Binding stoichiometry of all engineered Rac1 proteins was found to range between 0.7 and 0.9 mol of GTPγS/mol of Rac1 protein (Table 1); thus, differences in NADPH oxidase activation potency, among mutated Rac1 proteins, cannot be attributed to differences in GTPγS binding capability.

It can, therefore, be assumed that mutations in Rac1, as detailed in Table 1, caused local structural changes in specific domains or single residues rather then major alterations in the tertiary structure and folding of the proteins. This assumption is supported by three-dimensional structure modeling of the Rac1 point mutations.

Effects of p47-phox and p67-phox Concentrations on Kinetic Parameters of Rac1 Proteins. The ability of Rac1 protein to activate the NADPH oxidase is customarily measured in a semirecombinant cell-free assay (*8*). The two main parameters used to define Rac activity are V_{max} and EC_{50}. In preliminary experiments, it was noted that these two parameters are markedly dependent on the concentrations of p47-*phox* and p67-*phox* in the NADPH oxidase cell-free assay. To establish the optimal conditions for the definition of active vs inactive forms of Rac1, we performed a set of experiments wherein the ability of Rac1 proteins to activate the NADPH oxidase was measured at different concentrations of p47-*phox* and p67-*phox* (Figure 2 and Table 2). WT Rac1, in the GTPγS-bound form, and the constitutively active mutant Rac1(G12V) were representatives of the active form of Rac1, whereas WT Rac1, in the GDPβS-bound form, and the N-terminal effector region mutant Rac1(Y40K) represented the inactive form of Rac1. At concentrations of p47-*phox* and p67-*phox* below 20 nM, inactive forms of Rac1 did not yield satisfactory saturation curves (data not shown). Results presented in Figure 2A and Table 2 indicate that, at 20 nM p47-*phox* and p67-*phox*, there were significant differences between active and inactive forms of Rac1 proteins, expressed in lower V_{max} and higher EC_{50} values of the inactive forms. Increasing the concentrations of p47-*phox* and p67-*phox* to 40 nM caused an elevation in the V_{max} of the inactive forms, with no effect on the V_{max} of the active forms (Figure 2B and Table 2). At 200 nM, differences in V_{max} diminished, and yet inactive forms of Rac1 still possessed EC_{50} values higher than those of the active forms (Figure 2C and Table 2).

The above results suggest that it is possible to partially overcome the loss of Rac1 function by increasing the concentrations of p47-*phox* and p67-*phox* in the cell-free assay. Therefore, to maximize the difference between active and inactive forms of Rac1 proteins described in this report, the cell-free assays were performed at 20 nM p47-*phox* and p67-*phox*.

Effects of Domain Substitution in Rac1 on NADPH Oxidase Activation. The ability of Rac1 chimeric proteins (Table 1) to support O_2^- production was examined in the cell-free assay, as described in Experimental Procedures.

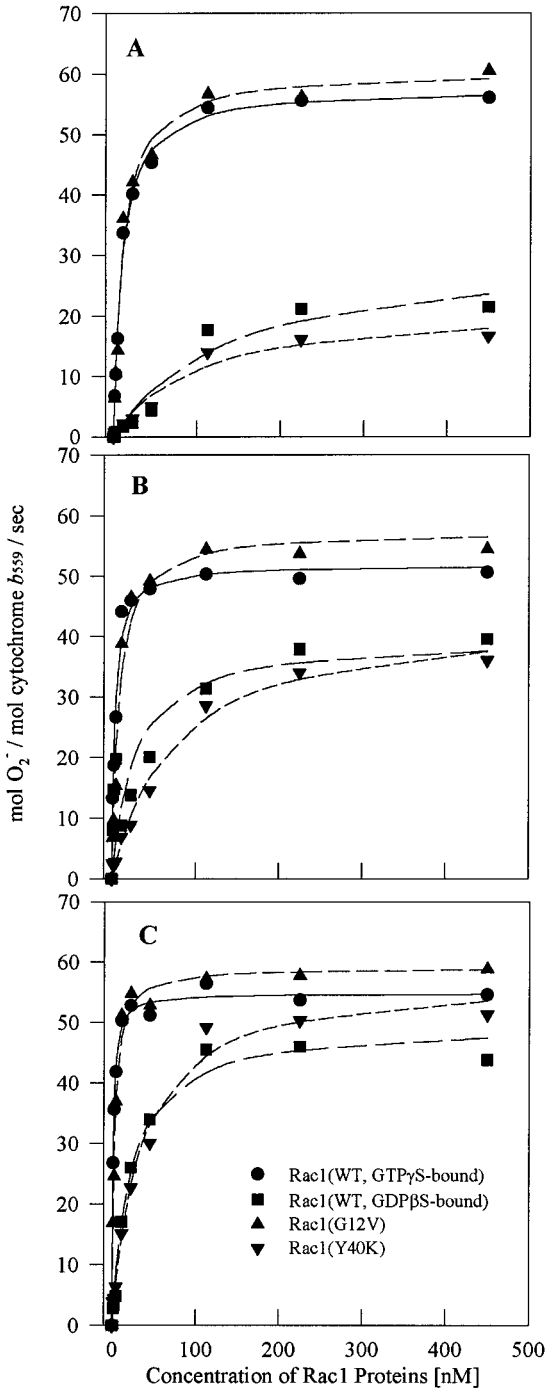

FIGURE 2: Effect of the concentration of p47-*phox* and p67-*phox* on the ability of Rac1 proteins to activate the NADPH oxidase. Rac1 proteins were assayed for their ability to stimulate O_2^- production in an amphiphile-activated cell-free assay. The reaction mixtures contained solubilized macrophage membranes (5 nM cytochrome b_{559}), in all panels; p47-*phox* and p67-*phox* at 20 nM (A), 40 nM (B), and 200 nM (C); varying concentrations of Rac1 proteins, as indicated on the abscissa (all panels), and assay buffer containing 130 μM LiDS and 200 μM cytochrome *c*, in a total volume of 200 μL. O_2^- production was initiated after 90 s of incubation by the addition of NADPH (250 μM). Rac1 proteins were preloaded with either GTPγS or GDPβS, by incubation for 30 min at 30 °C with a 20-fold molar excess of the nonhydrolyzable nucleotide analogues. O_2^- production was quantified by cytochrome *c* reduction. Low rates of O_2^- production, seen in the absence of Rac1 proteins, were subtracted from the rates obtained in the presence of Rac1 proteins. Data shown are means of triplicates and represent at least four experiments.

Rac1 proteins with substitutions in domain ***b*** ($_{103}$HH-CPN$_{107}$) [Rac1(***b*** → H-Ras) and Rac1(***b*** → GAGAG)] showed a markedly reduced ability to activate the NADPH oxidase in the cell-free assay (Figure 3A and Table 3). Substitution of this domain for its equivalent amino acid sequence in H-Ras (VKDSDD) creates a negatively charged region in Rac1 that could participate in nonspecific interactions. This substitution also resulted in the insertion of an additional amino acid into the protein (five amino acids were replaced by six). To eliminate the possible effect of these changes, domain ***b*** was substituted for a stretch of five small uncharged residues (GAGAG). Although Rac1(***b*** → GAGAG) showed a slightly higher activity than the Rac1(***b*** → H-Ras) chimera, both proteins exhibited a significantly reduced ability to activate NADPH oxidase. This indicates that loss of activity of these proteins is not due to the insertion of the foreign domains but rather to the elimination of the Rac1-specific amino acid sequence.

Domain ***c*** ($_{123}$KDTIEKLKEKK$_{133}$) is part of the unique insert region (*53*) characteristic for the Rho subfamily (*40*). Deletion of this domain from Rac1 [Rac1(Δ***c***)] had only a slight effect on the ability of the protein to activate NADPH oxidase in the cell-free system (Figure 3B and Table 3). Thus, the V_{max} of the deletion mutant [Rac1(Δ***c***)] was identical to that of native Rac1 protein, whereas the EC_{50} was only slightly higher.

Domain ***d*** ($_{163}$RGLKTV$_{168}$), at the C-terminus of Rac1, was substituted for its equivalent domain in H-Ras (QGVE-DA). The resulting chimera [Rac1(***d*** → H-Ras)] was a poor activator of NADPH oxidase (Figure 3C and Table 3). The substitution of the amino acid sequence in this domain was done strictly in accordance with the structural alignment of H-Ras and Rac1, based on the X-ray-solved three-dimensional structure of Rac1 (*53*), and therefore the impaired activity of this chimera is, most likely, due to the elimination of the amino acid sequence of Rac1 domain ***d***.

As a control for substitutions of specific domains, identified by "peptide walking" as participating in the activation of NADPH oxidase, the $_{135}$TPITYP$_{140}$ sequence (designated ***control*** domain), for which there was no evidence for involvement in NADPH oxidase activation, was substituted for its equivalent in H-Ras (RTVESR). As shown in Figure 3D and Table 3, the resulting chimera [Rac1(***control*** → H-Ras)] exhibited only a minimal increase in EC_{50} and a V_{max} identical to that of native Rac1 protein.

Testing the ability of chimeric proteins to activate NADPH oxidase in a cell-free assay containing concentrations of p47-*phox* and p67-*phox* higher than 20 nM revealed that, under these conditions, domain ***b*** and ***d*** chimeras essentially maintained their distinctive kinetic parameters (both V_{max} and EC_{50}), whereas the minimal changes in kinetic parameters exhibited by domain ***c*** and ***control*** domain chimeras were further diminished (data not shown).

Effects of Point Mutations, within Selected Rac1 Domains, on NADPH Oxidase Activation. To define the role of single amino acids in determining the functional significance of domains ***b*** and ***d***, a series of point mutations were generated within these domains, as detailed in Table 1.

The following single amino acid mutations were introduced into domain ***b***: H103A, H104A, C105A, and N107D. Mutating H103, the most exposed amino acid in this domain, significantly reduced the ability of Rac1 to activate the

Table 2: Effect of p47-*phox* and p67-*phox* Concentrations on Kinetic Parameters of Rac1 Proteins[a]

	concentration of p47-*phox* and p67-*phox*					
	20 nM		40 nM		200 nM	
kinetic parameters of Rac1 proteins	EC_{50} (nM)	V_{max} [mol of O_2^- (mol of cytochrome b_{559})$^{-1}$ s^{-1}]	EC_{50} (nM)	V_{max} [mol of O_2^- (mol of cytochrome b_{559})$^{-1}$ s^{-1}]	EC_{50} (nM)	V_{max} [mol of O_2^- (mol of cytochrome b_{559})$^{-1}$ s^{-1}]
Rac1(WT-GTPγS)	10.1 ± 1.1[b]	60 ± 2[b]	3.0 ± 0.8	57 ± 2	1.1 ± 0.1	57 ± 1
Rac1(WT-GDPβS)[c]	161.0 ± 21.0	28 ± 8	54.3 ± 2.7	45 ± 5	11.5 ± 4.2	56 ± 4
Rac1(G12V)	11.8 ± 3.1	61 ± 1	5.7 ± 0.9	55 ± 1	2.4 ± 0.3	55 ± 4
Rac1(Y40K)	97.6 ± 9.2	22 ± 8	56.8 ± 15.0	46 ± 2	24.9 ± 8.1	58 ± 1

[a] LiDS-elicited O_2^- production assays were performed as described in the legend to Figure 2. Kinetic parameters of Rac1 proteins were determined as described in Experimental Procedures. [b] Data represent the mean of at least four experiments ± SEM, from three individual preparations of NADPH oxidase components. [c] The WT Rac1 was tested both in its GTPγS- and GDPβS-bound forms; the Rac1 mutants were tested exclusively in their GTPγS-bound form. Nucleotide preloading of Rac1 proteins was performed as described in Experimental Procedures.

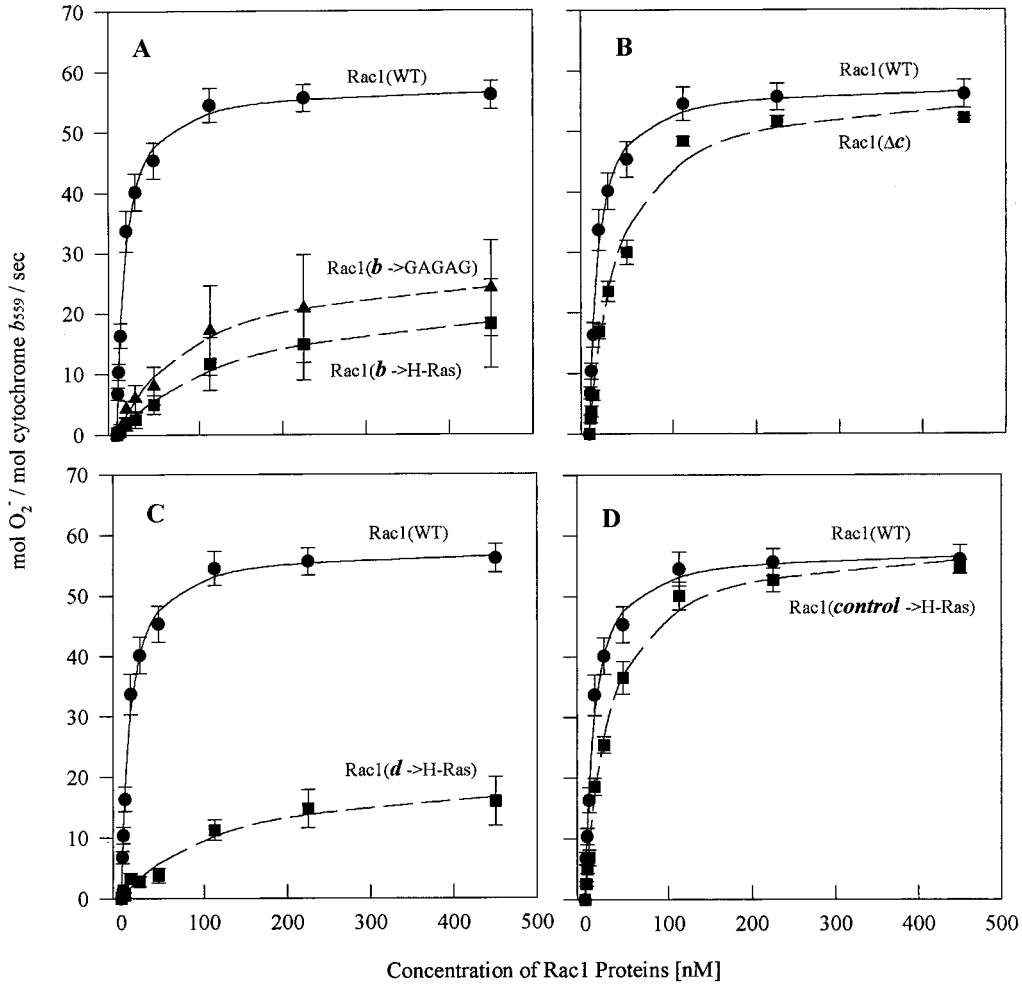

FIGURE 3: Comparison between native Rac1 and Rac1/H-Ras chimeric proteins, in activation of the NADPH oxidase. Domains in the Rac1 protein were substituted with the corresponding regions of H-Ras protein, as detailed in Table 1. The chimeric proteins were tested for their ability to stimulate O_2^- production in the semirecombinant cell-free assay, performed as described in Experimental Procedures. The concentration of p47-*phox* and p67-*phox* was 20 nM. Proteins were preloaded with GTPγS, as described in Experimental Procedures. WT Rac1 appears in all panels for the purpose of comparison. Bars represents means ± SEM from at least five experiments, using proteins from at least three individual preparations.

NADPH oxidase. This was expressed in both a lower V_{max} and a marked increase in EC_{50}. Point mutations H104A, C105A, and N107D had less pronounced effects on Rac1 function, reflected mainly in higher EC_{50} values (Figure 4A and Table 3).

Three point mutations were generated in domain ***d***, focused on the nonconservative residue substitutions present in the Rac1(***d*** → H-Ras) chimera: R163D, K166E, and T167E. Rac1 mutants R163D and T167E, as opposed to point mutations in domain ***b***, exhibited kinetic parameters indistinguishable from those of native Rac1, both in their V_{max} and EC_{50}. On the other hand, mutation K166E resulted in a pronounced decrease in Rac1 activity, as expressed by a lower V_{max} and a markedly elevated EC_{50} (Figure 4B and Table 3).

Similarly to the inactive forms of Rac1 (GDP-bound WT and Y40K mutant), the loss of NADPH oxidase activating ability by the H103A and K166E mutants could be partially

Table 3: Kinetic Parameters of Rac1 Proteins[a]

proteins	Rac1 EC_{50} (nM)	Rac1 V_{max} [mol of O_2^- (mol of cytochrome b_{559})$^{-1}$ s^{-1}]
Rac1(WT)	10.1 ± 1.1[b]	60 ± 2[b]
Rac1(G12V)	11.8 ± 3.1	61 ± 1
Rac1(Y40K)	97.6 ± 9.2	22 ± 8
Rac1(***b*** → H-Ras)	149.0 ± 11.0	24 ± 9
Rac1(***b*** → GAGAG)	95.8 ± 9.7	31 ± 7
Rac1(H103A)	87.9 ± 8.7	31 ± 5
Rac1(H104A)	41.4 ± 5.0	58 ± 1
Rac1(C105A)	44.4 ± 1.5	59 ± 4
Rac1(N107D)	52.2 ± 7.2	58 ± 2
Rac1(Δ***c***)	33.2 ± 4.5	58 ± 1
Rac1(***d*** → H-Ras)	123.0 ± 14.0	24 ± 9
Rac1(R163D)	12.5 ± 1.1	57 ± 1
Rac1(K166E)	78.4 ± 8.5	40 ± 4
Rac1(T167E)	15.0 ± 1.9	59 ± 2
Rac1(***control*** → H-Ras)	27.2 ± 2.6	58 ± 2

[a] Rac1 proteins (WT and mutants) were generated and expressed as described in Experimental Procedures. O_2^- production assays were performed and kinetic parameters were determined as described in Experimental Procedures. The concentration of p47-*phox* and p67-*phox* in the assays was 20 nM. All Rac1 proteins were preloaded with GTPγS as described in Experimental Procedures. [b] Data represent the mean of at least five experiments ± SEM from at least three individual protein purifications.

overcome by increasing the concentrations of p47-*phox* and p67-*phox* in the cell-free assay (data not shown).

DISCUSSION

The notion that small GTP binding proteins possess additonal effector domains, downstream of the well-defined N-terminal effector site (residues 26−48), is gradually acquiring acceptance, supported by a steady accumulation of experimental data. Studies using Ras/Rho chimeric proteins suggested that Rho proteins contain a second functionally important effector site, C-terminal to residue 69 (*60*). The application of "peptide walking" to Rac1 revealed four previously unidentified domains (***a***−***d***) in the C-terminal two-thirds of the molecule, essential for supporting NADPH oxidase activation in vitro (*45*). These results required confirmation by other methodologies because peptides might act in a nonspecific, sequence-independent manner. Also, "peptide walking" is not appropriate for identifying essential single residues. Thus, construction of chimeric proteins, domain deletion, and single amino acid mutagenesis were used to confirm and complement results obtained by peptide scanning. We found that the mutagenesis-based methods yielded results in good agreement with the predictions derived from "peptide walking" for domains ***b*** and ***d*** but could not confirm the relevance of domain ***c***.

Domain ***b*** consists of the two C-cap residues of α helix 3 and a turn (type II) connecting the helix to β strand S5. H103 is exposed on the surface of the molecule and the side chains of both residues H103 and H104 are stabilized by a network of ring−ring interactions involving P69 and Y72 (Figure 5a). The latter residues are located in a region that is highly conserved in the Rho subfamily and were found to be involved in the mediation of conformational changes (*61*) and intermolecular interactions (*62*, *63*) in proteins of the Ras superfamily. Models for the mutants H103A (Figure 5b), H104A, C105A, and N107D suggest that all mutations are easily accommodated in the structure, resulting in small

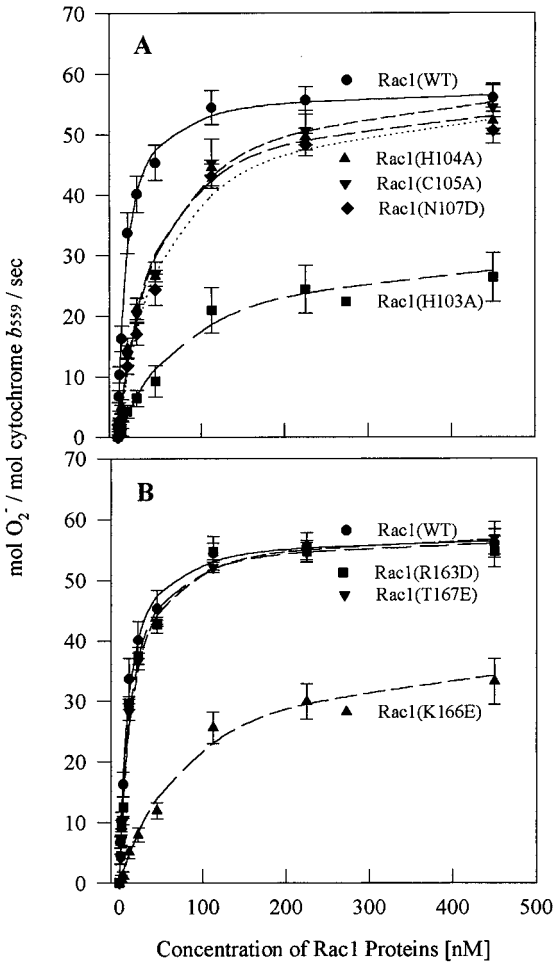

FIGURE 4: Effect of point mutations within domains ***b*** and ***d*** on the ability of Rac1 proteins to activate the NADPH oxidase. Selected amino acids, within domains ***b*** and ***d***, were mutated, as detailed in Table 1. The Rac1 proteins carrying point mutations were tested for their ability to stimulate O_2^- production in the semirecombinant cell-free assay. Experimental conditions were as described in the caption to Figure 3. WT Rac1 appears in both panels for the purpose of comparison. Bars represents means ± SEM from at least five experiments, using proteins from at least three individual preparations.

local changes without disrupting the overall fold of Rac1, the ring−ring interactions (except that between H103 and H104), and the conformation of residues that interact with the nucleotide. Substitution of domain ***b*** for non-Rac sequences and the point mutation H103A reduced significantly the ability of the protein to activate the NADPH oxidase. Comparison between the GTP- and GDP-bound forms of Rac1 showed domain ***b*** to adopt different conformations depending on the nature of the bound nucleotide (M. Hirshberg, L. Lloyd-Haire, and M. Webb, unpublished results). This was also proposed for the analogous region in Ras (*64*−*66*), making it a candidate for interaction with target molecules. Domain ***b*** was not identified before to be important for NADPH oxidase activation by chimeric protein or site-directed mutagenesis approaches; however, analogous regions in other GTP binding proteins were shown to be of functional relevance. This region was found to serve as an important interaction motif in c-H-Ras (*67*, *62*), the Rab family (*68*, *63*), the yeast GTPases Ypt and Sec4 (*69*, *70*), and in the α subunit of the trimeric GTP binding protein Gs (*71*).

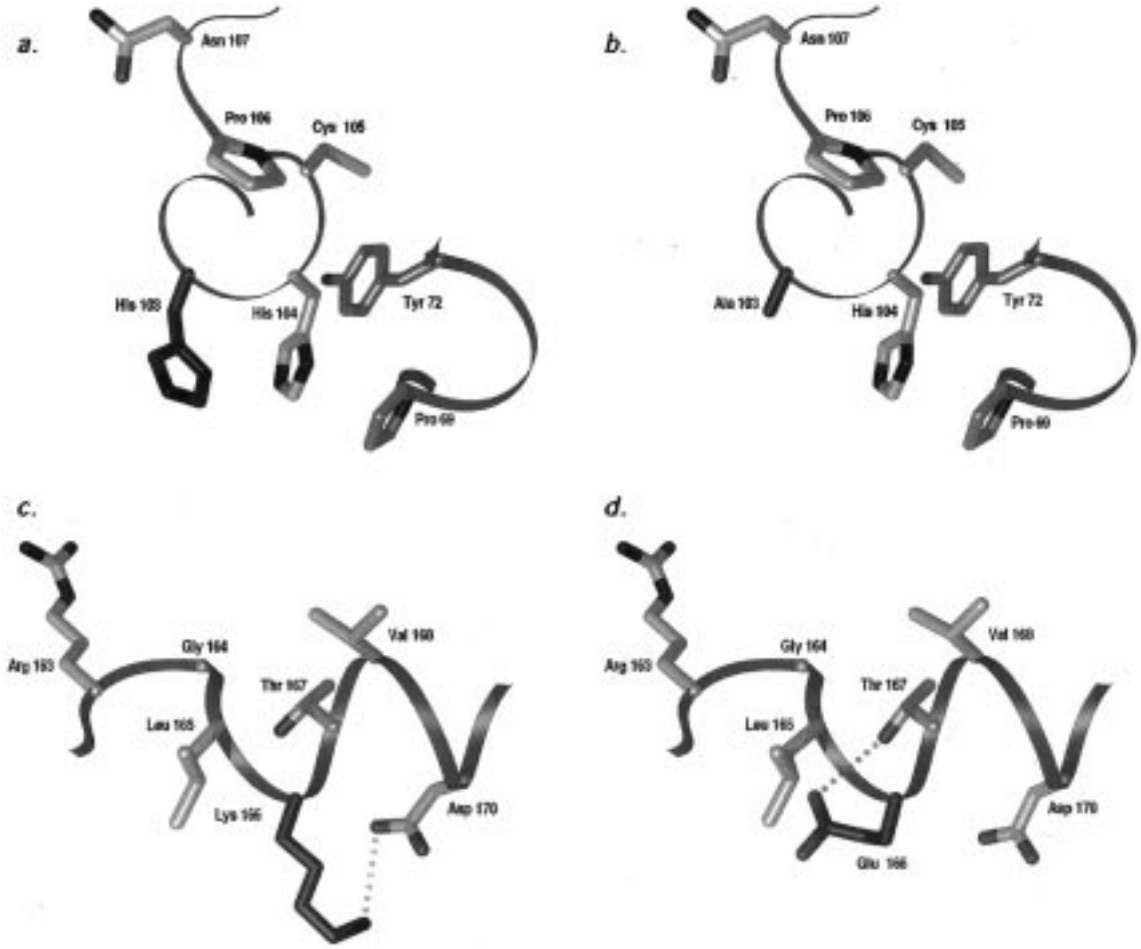

FIGURE 5: Stick representation of domains ***b*** and ***d*** in Rac1. Panels a and b show WT and H103A mutant, respectively, of domain ***b*** ($_{103}$HHCPN$_{107}$) as well as residues P69 and Y72, which take part in ring−ring stabilization interactions. Panels c and d show WT and K166E mutant of domain ***d*** ($_{163}$RGLKTV$_{168}$), respectively. Nitrogen, oxygen, and sulfur atoms are colored in blue, red, and yellow, respectively. Carbon atoms of residues 103 and 166 are colored in green, and those of residues 72 and 69, in magenta. Hydrogen bonds are represented by dotted gray lines. The figure was generated with Bobscript (*74*).

Domain ***c*** is part of the insert region extending from L117 to I137 and consists of two α helices, H3a and H3b, followed by an extended loop. This region is characteristic for the Rho subfamily, and the corresponding structure in H-Ras is a short loop (*53*). In Cdc42Hs, this region is involved in binding to the GTPase activating proteins (GAPs) IQGAP1 and IQGAP2 (*72*) and is required for inhibition of GDP dissociation and GTP hydrolysis by RhoGDI (*73*). The insert region was proposed to play a role in the NADPH oxidase activating function of Rac1 on the basis of "peptide walking" experiments (*45*), in which it was found that peptides sharing a domain consisting of residues 123−133 inhibited Rac1-dependent O_2^- production in the cell-free system. We found that a deletion mutant lacking residues 123−133, which eliminates the α helix H3b and the two N-cap residues of the following loop, exhibited only a minor reduction in its ability to activate NADPH oxidase. Our finding of an essentially unaltered NADPH oxidase activating capacity of the domain ***c*** deletion mutant is in good agreement with results obtained with Rac1/Cdc42Hs (*38*) and Rac1/RhoA (*39*) chimeric proteins, showing that substitution of a domain containing the insert region of Rac1 by domains containing the insert regions of Cdc42Hs or RhoA does not affect the NADPH oxidase activating ability of the chimeras. On the other hand, our results do not fulfill the predictions of "peptide walking", having led to the definition of domain ***c***. It should, however, be noted that peptides corresponding to domain ***c*** were much less inhibitory than peptides corresponding to domains ***b*** and ***d***, as reflected in higher IC_{50} values (*45*). Furthermore, "peptide walking" was performed with Rac1 in complex with RhoGDI and the fact that the insert region serves as a functional target for RhoGDI (*73*) raises the possibility that domain ***c*** peptides interfered with a step in NADPH oxidase activation involving the Rac1−RhoGDI dimer. This would not be detected in work with the domain ***c*** deletion mutant, which is assayed in the absence of RhoGDI. Finally, peptides corresponding to domain ***c*** contain a high proportion of basic residues and it is possible that their inhibitory effect was not sequence-specific but charge-related. Such a nonspecific inhibitory effect of polybasic peptides on NADPH oxidase activation was recently observed (*43*).

Our findings differ from those of Lambeth and colleagues (*41*, *34*). These authors reported recently that deletion of residues 124−135 in Rac1 and several point mutations in this region resulted in mutants with markedly diminished NADPH oxidase activating ability (*41*) but an unchanged binding affinity for p67-*phox* (*34*). There are a number of differences in the design and methodology of the experiments as performed by us and by Lambeth and colleagues. These are as follows: (1) The limits of the deleted domains are different: residues 123−133, in our mutant, versus residues

124−135, in the mutant described in ref *41*. Therefore, our deletion includes E127, K130, and K132, mutations of which were reported by Lambeth's group to compromise the ability of Rac1 to activate NADPH oxidase, but does not include L134 and T135, two residues found by the same authors to be of comparable importance to the first three. (2) Deletion mutant 124−135 contains two additional point mutations, one adjacent to the deletion (P136A) and one at the C-terminus (C189S). (3) The membrane preparation used in our assay is guinea pig macrophage-derived and solubilized, whereas that used by Lambeth's group is human neutrophil-derived and unsolubilized. (4) The cell-free assay techniques employed in the two laboratories differ in the concentrations of the NADPH oxidase components present in the assay and in the nature of and conditions of exposure to the activating amphiphile. We are not able to conclude which, if any, of these differences offers the explanation for the discrepant results, and further work on this domain, by alternative approaches, is definitely justified.

Domain ***d*** consists of the end of turn (type II) connecting β strand S5 and the amino end of α helix H5. It is located between the GTP base recognition motif $_{158}$SAL$_{160}$ and the polybasic motif at the carboxyl tail of Rac1. The side chains of all residues but the hydrophobic ones (L165 and V168) are relatively exposed. It can be deduced from the Rac1 structure that the side chains of residues R163 and K166 are hydrogen-bonded to the side chains of residues D121 and D170, respectively (Figure 5c). Modeling of mutant R163D, K166E, and T167E suggests that these are easily accommodated in the Rac1 fold with only small local structural perturbations, which do not influence the nucleotide binding residues. In the K166E mutant, the hydrogen bond between the side chains of residues 166 and 170 is lost, and E166 forms a hydrogen bond with T167 (Figure 5d). The Rac1(***d*** → H-Ras) chimera and the point mutant K166E had a significantly reduced NADPH oxidase activating potency. It is likely that the C-terminal effector region (residues 143−175), as described by Diekmann et al. (*39*), represents a less rigorously defined version of domain ***d***, the limits of which were determined by "peptide walking". Our present results provide further information on this domain by demonstrating the crucial role of K166 in the activation of NADPH oxidase by Rac1.

In conclusion, examination of the three-dimensional structure of Rac1 reveals that residues H103, in domain ***b***, and K166, in domain ***d***, are exposed on the surface of the molecule. Structural analysis of domains ***b*** and ***d*** point mutations suggests that the effect (or lack of effect) of each mutation on NADPH oxidase activity depends on the particular side chains of the residues involved and not on larger structural changes induced by the mutation.

As only Rac proteins and neither RhoA nor Cdc42Hs are capable of significant activation of the NADPH oxidase (*38*, *39*), we made a comparative study of molecular models of domains ***b*** and ***d*** in these proteins. Sequence alignment of members of the Rho subfamily shows that both domains consist of conserved residues, in particular H103, which is conserved among all members of the Rho subfamily (alignment not shown). Comparison of the three-dimensional structures and electrostatic surfaces within each domain showed the domains to be very similar, exhibiting only small differences, which might be due to inaccuracy in model building. Our experimental results, together with deductions based on modeling, permit two interpretations for the specificity of Rac1 as an activator of the NADPH oxidase. In the first, H103 and K166 are identified as essential residues in the oxidase activating function of Rac1 and the small differences between domains ***b*** and ***d*** in Rac1 and the other Rho subfamily proteins are important contributors to the specificity of Rac1. In the second interpretation, H103 and K166 are seen as being required for NADPH oxidase activation, but residues located in the N-terminal effector loop (*38*) are responsible for the exclusivity of Rac1 as an NADPH oxidase activator. Our results are in general agreement with the model proposed by Nisimoto et al. (*34*), in which various functional domains exposed on the surface of Rac1 are seen to interact with distinct NADPH oxidase components. It is also possible that more than one Rac1 domain is involved in interaction with multiple domains on a single NADPH oxidase component. The identity of the component(s) interacting with domains ***b*** and ***d*** on Rac1 remains to be determined by direct binding experiments.

In summary, we present further evidence for the involvement of two effector sites, located in the C-terminal half of Rac1, in the activation of NADPH oxidase, in addition to that located in the N-terminal region. The multiplicity of effector domains might serve one of the following purposes: interaction with more than one NADPH oxidase component; an increase in the affinity of binding to a single component, or engagement in a temporal sequence of interactions, as NADPH oxidase assembly progresses.

ACKNOWLEDGMENT

We thank Dr. T. L. Leto (National Institutes of Health, Bethesda, MD) for providing baculoviruses carrying cDNAs for p47-*phox* and p67-*phox* and Rac1 plasmid in *E. coli*.

REFERENCES

1. Morel, F., Doussiere, J., and Vignais, P. V. (1991) *Eur. J. Biochem. 201*, 523−546.
2. Segal, A. W., and Abo, A. (1993) *Trends Biochem. Sci. 18*, 43−47.
3. Robinson, J. M., and Badwey, J. A. (1995) *Histochemistry 103*, 163−180.
4. DeLeo, F. R., and Quinn, M. T. (1996) *J. Leukocyte Biol. 60*, 677−691.
5. Bromberg, Y., and Pick, E. (1984) *Cell. Immunol. 88*, 213−221.
6. Bromberg, Y., and Pick, E. (1985) *J. Biol. Chem. 260*, 13539−13545.
7. Rotrosen, D., Yeung, C. L., Leto, T. L., Malech, H. L., and Kwong, C. H. (1992) *Science 256*, 1459−1462.
8. Abo, A., Boyhan, A., West, I., Thrasher, A. J., and Segal, A. W. (1992) *J. Biol. Chem. 267*, 16767−16770.
9. Thrasher, A. J., Keep, N. H., Wientjes, F., and Segal, A. W. (1994) *Biochim. Biophys. Acta 1227*, 1−24.
10. Abo, A., and Pick, E. (1991) *J. Biol. Chem. 266*, 23577−23585.
11. Seifert, R., Rosenthal, W., and Schultz, G. (1986) *FEBS Lett. 205*, 161−165.
12. Gabig, T. G., English, D., Akard, L. P., and Schell, M. J. (1987) *J. Biol. Chem. 262*, 1685−1690.
13. Ligeti, E., Tardif, M., and Vignais, P. V. (1989) *Biochemistry 28*, 7116−7123.
14. Abo, A., Pick, E., Hall, A., Totty, N., Teahan, C. G., and Segal, A. W. (1991) *Nature 353*, 668−670.
15. Knaus, U. J., Heyworth, P. G., Evans, T., Curnutte, J. T., and Bokoch, G. M. (1991) *Science 254*, 1512−1515.

16. Mizuno, T., Kaibuchi, K., Ando, S., Musha, T., Hiraoka, K., Takaaishi, K., Asada, M., Nunoi, H., Matsuda, I., and Takai, Y. (1992) *J. Biol. Chem. 267*, 10215−10218.
17. Kwong, C. H., Malech, H. L., Rotrosen, D., and Leto, T. L. (1993) *Biochemistry 32*, 5711−5717.
18. Polakis, P. G., Weber, R. F., Nevins, B., Didsbury, J. R., Evans, T., and Snyderman, R. (1989) *J. Biol. Chem. 264*, 16383−16389.
19. Pick, E., Gorzalczany, Y., and Engel, S. (1993) *Eur. J. Biochem. 217*, 441−455.
20. Knaus, U. G., Heyworth, P. G., Kinsella, B. T., Curnutte, J. T., and Bokoch, G. M. (1992) *J. Biol. Chem. 267*, 23575−23582.
21. Quinn, M. T., Evans, T., Loetterle, L. R., Jesaitis, A. J., and Bokoch, G. M. (1993) *J. Biol. Chem. 268*, 20983−20987.
22. Abo, A., Webb, M. R., Grogan, A., and Segal, A. W. (1994) *Biochem. J. 298*, 585−591.
23. Le Cabec, V., Mohn, H., Gacon, G., and Maridonneau-Parini, I. (1994) *Biochem. Biophys. Res. Commun. 198*, 1216−1224.
24. Philips, M. R., Feoktistov, A., Pillinger, M. H., and Abramson, S. B. (1995) *J. Biol. Chem. 270*, 11514−11521.
25. Dusi, S., Donini, M., and Rossi, F. (1995) *Biochem. J. 308*, 991−994.
26. Dusi, S., Donini, M., and Rossi, F. (1996) *Biochem. J. 314*, 409−412.
27. Leusen, J. H. W., De Klein, A., Hilarius, P. M., Ahlin, A., Palmblad, J., Smith, C. I. E., Diekmann, D., Hall, A., Verhoeven, A. J., and Roos, D. (1996) *J. Exp. Med. 184*, 1243−1249.
28. Heyworth, P. G., Bohl, B. P., Bokoch, G. M., and Curnutte, J. T. (1994) *J. Biol. Chem. 269*, 30749−30752.
29. Kleinberg, M. E., Malech, H. L., Mital, D. A., and Leto, T. L. (1994) *Biochemistry 33*, 2490−2495.
30. Dorseuil, O., Quinn, M. T., and Bokoch, G. M. (1995) *J. Leukocyte Biol. 58*, 108−113.
31. Diekmann, D., Abo, A., Johnston, C., Segal, A. W., and Hall, A. (1994) *Science 265*, 531−533.
32. Prigmore, E., Ahmed, S., Best, A., Kozma, R., Manser, E., Segal, A. W., and Lim, L. (1995) *J. Biol. Chem. 270*, 10717−10722.
33. Dorseuil, O., Reibel, L., Bokoch, G. M., Camonis, J., and Gacon, G. (1996) *J. Biol. Chem. 271*, 83−88.
34. Nisimoto, Y., Freeman, J. L. R., Motalebi, S. A., Hirshberg, M., and Lambeth, J. D. (1997) *J. Biol. Chem. 272*, 18834−18841.
35. Wittinghofer, A., and Nassar, N. (1996) *Trends Biochem. Sci. 21*, 488−491.
36. Xu, X., Barry, D. C., Settleman, J., Schwartz, M. A., and Bokoch, G. M. (1994) *J. Biol. Chem. 269*, 23569−23574.
37. Freeman, J. L. R., Kreck, M. L., Uhlinger, D. J., and Lambeth J. D. (1994) *Biochemistry 33*, 13431−13435.
38. Kwong, C. H., Adams, A. G., and Leto, T. L. (1995) *J. Biol. Chem. 270*, 19868−19872.
39. Diekmann, D., Nobes, C. D., Burbelo, P. D., Abo, A., and Hall, A. (1995) *EMBO J. 14*, 5297−5305.
40. Valencia, A., Chardin, P., Wittinghofer, A., and Sander, C. (1991) *Biochemistry 30*, 4637−4648.
41. Freeman, J. L., Abo, A., and Lambeth, J. D. (1996) *J. Biol. Chem. 271*, 19794−19801.
42. Kreck, M. L., Uhlinger, D. J., Tyagi, S. R., Inge, K. L., and Lambeth, J. D. (1993) *J. Biol. Chem. 269*, 4161−4168.
43. Joseph, G., Gorzalczany, Y., Koshkin, V., and Pick, E. (1994) *J. Biol. Chem. 269*, 29024−29031.
44. Kreck, M. L., Freeman, J. L., Abo, A., and Lambeth, J. D. (1996) *Biochemistry 35*, 15683−15692.
45. Joseph, G., and Pick, E. (1995) *J. Biol. Chem. 270*, 29079−29082.
46. Cormack, B. (1991) Mutagenesis by the polymerase chain reaction, in *Current Protocols in Molecular Biology* (Ausubel, F. M., Brent, R., Kingston, R. E., Moore, D. D., Seidman, J. G., Smith, J. A., and Struhl, K., Eds.) pp 8.5.1−8.5.9, John Wiley & Sons, New York.
47. Knoller, S., Shpungin, S., and Pick, E. (1991) *J. Biol. Chem. 266*, 2795−2804.
48. Diatchuk, V., Lotan, O., Koshkin, V., Wikstroem, P., and Pick, E. (1997) *J. Biol. Chem. 272*, 13292−13301.
49. Leto, T. L., Garrett, M. C., Fujii, H., and Nunoi, H. (1991) *J. Biol. Chem. 266*, 19812−19818.
50. Northup, J. K., Smigel, M. D., and Gilman, A. C. (1982) *J. Biol. Chem. 257*, 11416−11423.
51. Bokoch, G. M., and Quilliam, L. A. (1990) *Biochem. J. 267*, 407−411.
52. Bradford, M. M. (1976) *Anal. Biochem. 72*, 248−254.
53. Hirshberg, M., Stockley, R. W., Dodson, G., and Webb, M. R. (1977) *Nat. Struct. Biol. 4*, 147−152.
54. Lee, C., and Subbiah, S. (1991) *J. Mol. Biol. 217*, 373−388.
55. Levitt, M. (1988) *Proc. Natl. Acad. Sci. U.S.A. 85*, 7557−7561.
56. LOOK: An Integrated Package for Sequence Analysis, Model Building and Function Determination (1994) Molecular Application Group, Palo Alto, CA.
57. Rittinger, K., Walker, P. A., Eccleston, J. F., Nurmahomed, K., Owen, D., Laue, E., Gamblin, S. J., and Smerdon, S. J. (1997) *Nature 388*, 693−697.
58. Rittinger, K., Walker, P. A., Eccleston, J. F., Smerdon, S. J., and Gamblin, S. J. (1997) *Nature 389*, 758−762.
59. Barnard, D., Diaz, B., Hettich, L., Chuang, E., Zhang, X.-F., Avruch, J., and Marshall, M. (1995) *Oncogene 10*, 1283−1290.
60. Self, A. J., Paterson, H. F., and Hall, A. (1993) *Oncogene 8*, 655−661.
61. Ma, J., and Karplus, M. (1997) *Proc. Natl. Acad. Sci. U.S.A. 94*, 11905−11910.
62. Segal, M., Marbach, I., Willumsen B. M., and Levitzki, A. (1995) *Eur. J. Biochem.* 228, 96−101.
63. Stenmark, H., Valencia, A., Martinez, O., Ullrich, O., Goud, B., and Zerial, M. (1994) *EMBO J. 13*, 575−583.
64. Stouten, P. F. W., Sander, C., Wittinghofer, A., and Valencia, A. (1993) *FEBS Lett. 320*, 1−6.
65. Hu, J.-S., and Redfield, A. G. (1993) *Biochemistry 32*, 6763−6772.
66. Diaz, J. F., Wroblowski, B., and Engelborghs, Y. (1995) *Biochemistry 34*, 12038−12047.
67. Willumsen B. M., Vass, W. C., Velu, T. J., Papageorge, A. J., Schiller, J. T., and Lowy, D. R. (1991) *Mol. Cell. Biol. 11*, 6029−6033.
68. Moore, I., Schell, J., and Palme, K. (1995) *Trends Biochem. Sci. 20*, 10−12.
69. Brennwald, P., and Novick, P. (1993) *Nature 362*, 560−563.
70. Dunn, B., Stearns, T., and Botstein, D. (1993) *Nature 362*, 563−565.
71. Berlot, C. H., and Bourne, H. R. (1992) *Cell 68*, 911−922.
72. McCallum, S. J., Wu, W. J., and Cerione, R. A. (1996) *J. Biol. Chem. 271*, 21732−21737.
73. Wu, W. J., Leonard, D. A., Cerione, R. A., and Manor, D. (1997) *J. Biol. Chem. 272*, 26153−26158.
74. Esnouf, R. M. (1997) *J. Mol. Graphics 15*, 133−138.

BI9800404